

An Approach of Constant False Alarm Ratio for Improved Target Tracking

Zvonko Radosavljević ¹⁾
Dejan Ivković ¹⁾

Each radar has the function of surveillance of certain areas of interest. In particular, the radar also has the function of tracking moving targets in that territory with some probability of detection, which depends on the type of detector. Constant false alarm ratio (CFAR) is a very commonly used detector. Changing the probability of target detection can directly affect the quality of tracking the moving targets. The paper presents the theoretical basis of the influence of CFAR detectors on the quality of tracking, as well as an approach to the selection of CFAR detectors, CATM CFAR, which enables better monitoring by the Interacting Multiple Model (IMM) algorithm with two motion models. Comparative analysis of CA and CATM algorithm realized by numerical simulations has shown that CATM CFAR gives less tracking error with proportionally the same computer resources.

Key words: Index Terms - CFAR detector, radar detection, IMM, target tracking.

Introduction

THE radar sensors have different sources of noise, so the detector in radar receivers has the adaptive threshold. Constant false alarm rate (CFAR) detectors are designed to track changes in the interference and to adjust the detection threshold to maintain a constant probability of the false alarm. Detection decisions are based on measurements of reflected signals received at the radar and thermal noise inherently presented in the receiver. The radar detector is tasked with comparing the measurement with a threshold and choosing between two hypotheses [1]:

- a) Measurements exceeding the threshold are declared to contain returns from the targets as well as the energy from interfering sources and are associated with the target-plus-interference hypothesis (commonly referred to as the H_1 hypothesis).
- b) Measurements below the threshold are declared to contain the energy only from the interfering sources and are associated with the null hypothesis, H_0 .

It must use the adaptive threshold detector, which has a feature that automatically adjusts its sensitivity according to a variety of interference power. Thus, it maintains a constant probability of the false alarm [2, 3].

An examination of CFAR algorithms begins with the cell-averaging (CA) CFAR. The CA-CFAR exhibits the optimum performance in a homogeneous interference environment.

They are used very often as a detector of very close targets per azimuth and per range using the Linear and Non Linear Fusion Constant False Alarm Rate (LF-CFAR and NLF-CFAR) detectors and single CA-CFAR (Cell Averaging CFAR), OS-CFAR (Ordered Statistic CFAR) and TM-CFAR (Trimmed Mean CFAR) which are considered in [5, 6].

When tracking targets in clutter, existence and position of the targets in the surveillance are a-priori unknown. Unknown

association of measurements with appropriate targets (unknown measurement source) is a common problem in multi target tracking. Automatic track initiation and termination under such conditions requires some knowledge about the track existence. A track exists if it is based on the measurements from a target (which follows specified dynamic and detection models), and is not a product of random clutter only. If a track follows a target, we shall call it a true track, otherwise we shall call it a false track.

A tracking algorithm named the Interacting Multiple Model (IMM) estimator, which provides tracking estimates with significant noise reduction and response to sequences of aircraft maneuver modes is introduced in [7]. The tracking of an object in a cluttered environment might be a challenge due to the several observations for a single aircraft under such environment [8]. That is, some tracking measurements do not originate from the target. Therefore, the present paper utilizes the Probabilistic Data Association filter (PDAF) [9] to assign weights to the validated measurements. We consider the problem of tracking multiple maneuvering targets from possibly missing and false measurements, with the aim to develop novel combinations of two well known approaches in target tracking: Interacting Multiple Model (IMM) algorithm and multi target versions of PDAF. Because each of these two solve complementary tracking problems it is of a significant interest to combine both approaches. The PDAF can extend the tracking capability to a highly cluttered environment. This paper combines the IMM estimator and PDAF to create an IMM-PDAF filter (IMM-PDAF), in order of improvement on the tracking performance [10].

Further, since sensor detection probability is generally below unity, it is also possible that no measurement on the target was received on a given scan. Pruning [3] involves either removing measurement histories with a low probability or removing whole sub-trees of the measurement histories.

¹⁾ Military Technical Institute (VTI), Ratka Resanovića 1, 11132 Belgrade, SERBIA
Correspondence to: Zvonko Radosavljević, e-mail: zvonko.radosavljevic@gmail.com

How different types of CFAR detectors influence the quality of targets tracking is the subject of the theoretical and experimental analysis in this paper. However, this topic is not often processed in the literature. Mostly, the targets clutter is treating only in the sense of radar and CFAR threshold [8], without review of tracking. This paper examines the effects of the two different CFAR detectors to the target tracking system.

The paper is organized as follows. After the introducing preamble, problem statements are presented in the Section II. The cell averaging (CA) and cell averaging-trimmed mean (CATM) CFAR detectors are briefly described at the beginning, in the Section III. The standard steps of the well-known IMM and PDAF algorithm are given in the Section IV. At the end of this Section, a probability of detection dependence on target tracking, followed by the results of simulation and final conclusions, from the Section V and Section VI, respectively.

Problem Statement

Consider the target tracking scenario with two dimensions. Target state is $[x \dot{x} y \dot{y}]$, where x, y are the Cartesian coordinates. Also, consider the tracking algorithm with two parameters: probability of detection (PD) and clutter density. The clutter density is depending on target dynamics and characteristics of the sensor. Generally, clutter is defined by a number of selection measurement from size of the selection gate. At the beginning, consider the target state $x_k \in R^{2z}$ at time interval k , which evolves according to:

$$x_k = Fx_{k-1} + v_k \quad (1)$$

where F is the state propagation matrix and the process noise, v_k is a zero mean and white Gaussian sequence with covariance matrix Q_k . The size of selection gate is depending on measurements matrix R and process noise matrix Q . False tracks are consumed at the beginning, while true tracks are depending on matrix Q . Measurement merging is best modelled in the sensor measurement space, while tracking and data association issues are using more often converted measurements. Converted target measurement $y \in R^{ny}$ is:

$$y_k = Hx_k + w_k \quad (2)$$

Clutter measurements follow the non-uniform Poisson distribution by clutter measurement density (Poisson intensity) ρ_y . At time k a set of $m(k)$ measurements

$Y(k) = \{y_i(k)\}_{i=1}^{m(k)}$ is detected, where each measurement either originates from one of n known linear measurement models or it is a false detection. The sequences $v(k)$ are mutually independent and uncorrelated with the process noise.

Description of CFAR algorithm

The basic parameters of each CFAR are the probability of false alarm rate P_{FA} , size of the window detection $N = 2n$, average signal value in cells Z , scaling factor of the detection threshold T and detection threshold S . Scaling factor of the detection threshold T is a constant which achieves a desired value of the probability of a false alarm for a given size of the window detection N . The detection window consists of two groups with the same number of cells n that are located on the opposite sides with respect to the cell whose contents are

tested. CFAR processes signals by averaging of signals in $2n$ neighbourhood range bins (X_i) and the resulting mean value compares with the signal in a range bin which is under the test (Y).

The cell averaging (CA) CFAR algorithm [4] consists of two collectors for the leading and lagging windows (Fig. 1). Here, Z is simply the sum of Y_1 and Y_2 . The cell Y in the middle of the reference window is a cell under test. Input samples are sent serially into the reference window. At the beginning, we calculate the mean clutter power level Z using the appropriate CFAR algorithm, and then we multiply Z by a scaling factor T which depends on the CFAR algorithm and the designed probability of the false alarm rate P_{fa} . Probability of detection P_{DCA} is given by [5]:

$$P_{DCA} = \left(1 + \frac{T}{1 + SNR}\right)^{-N} \quad (3)$$

where SNR is signal-to-noise ratio.

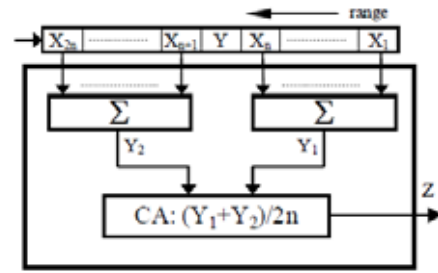


Figure 1. Block diagram CA-CFAR detector

The CATM-CFAR [4, 5] is a cell-averaging-trimmed-mean detector which optimizes the features of some mentioned CFAR detectors from different groups depending on the characteristics of the clutter and targets, and it is shown in Fig.2. The main goal of the CATM-CFAR modelling was increasing the probability of detection at a constant probability of the false alarm rate. The cell Y in the middle of the reference window is a cell under test. Input samples are sent serially into the reference window.

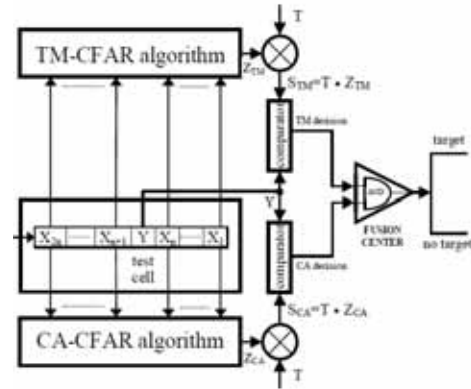


Figure 2. Block diagram of CATM-CFAR detector

The first step is to calculate the mean clutter power level Z using the appropriate CFAR algorithm. The second step is to multiply Z by a scaling factor T which depends on the CFAR algorithm and the designed probability of the false alarm rate P_{FA} . The product TZ is the detection threshold S . During this time, the TM-CFAR detector uses the first cells in the reference window to be sorted per amplitude. Then, it trims the T_1 smallest cells and T_2 cells with the highest amplitudes. After that, the summation of the content in the remaining cells is done to obtain Z . CATM CFAR algorithm is realized by the parallel. The CA CFAR detector and the TM CFAR detector

work simultaneously and independently but with the same scaling factor of the detection threshold T . They produce their own mean clutter power level Z using the appropriate $CFAR$ algorithm. Next, they calculate their own detection thresholds S_{CA} and S_{TM} . After the comparison with the content in the cell under the test Y , they decide about the target presence independently. The finite decision about target presence is made in the fusion center composed of one "and" logic circuit. If both input single decisions in the fusion center are positive, the finite decision of the fusion center is the presence of the target in the cell under the test. In other cases, the finite decision is negative and the target is not at the location which corresponds with the cell under the test. Probability of detection P_{DCATM} is given by [5]:

$$P_{DCATM} = \left(1 + \frac{T}{1 + SNR}\right)^{-N} \prod_{i=1}^{N-T_1-T_2} M_{V_i} \left(\frac{T}{1 + SNR}\right) \quad (4)$$

where M_V in (4) is defined as:

$$M_{V_i}(T) = \frac{N!}{T_1!(N-T_1-1)!(N-T_1-T_2)} \sum_{j=0}^{T_1} \frac{\binom{T_1}{j} (-1)^{T_1-j}}{\frac{N-j}{N-T_1-T_2} + T} \quad (5)$$

and

$$M_{V_i}(T) = \frac{a_i}{a_i + T}, \quad i = 2, 3, \dots, N - T_1 - T_2 \quad (6)$$

where a_i is defined as:

$$a_i = \frac{N - T_1 - i + 1}{N - T_1 - T_2 - i + 1} \quad (7)$$

Probability of detection of optimal CFAR detector

In radar signals processing it is not possible to use an optimal detector with the fixed optimal threshold S_O to decide the target existence, because is it a priori unknown background clutter. A solution is to use the $CFAR$ detector which has a constant probability of the false alarm. For the optimal detector with the fixed optimal threshold S_O , the probability of detection P_D is given by [4]:

$$P_D = P\{Y > S_O \mid H_1\} = \exp\left[-\frac{S_O}{2\mu(1 + SNR)}\right] \quad (8)$$

where H_1 is the hypothesis the target is present in the radar cell, parameter SNR signal to noise ratio and μ background clutter power. The corresponding diagram of dependence of probability of detection versus \hat{x}_{klk} signal-to-noise ratio SNR is given in Fig.3 according to (3), (4) and (8) for $N=16$ and $P_{fa}=10^{-6}$.

Finally, we have $CFAR$ probability of detection $-P_D^{CFAR}$ as follows [9]:

$$P_D = P\{\mathcal{X}_{k-1} \mid Z^{k-1}\} = \sum_{c=1}^{C_{k-1}} P\{\mathcal{X}_{k-1}^c \mid Z^{k-1}\} = P_D^{CFAR} \quad (9)$$

The set value of the signal-to-noise ratio (SNR) always gives a certain value of the detection probability P_D which is a parameter of the tracking quality. The parametric diagram (Fig.3) shows this dependence with a change in the probability of the false alarm.

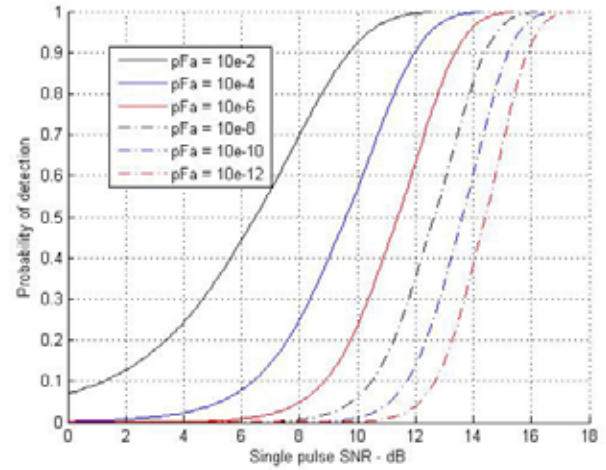


Figure 3. Parametric diagram probability of detection P_D versus SNR (parameter probability of false alarm P_{FA})

Interacting multiple model probabilistic data association filter

IMM algorithm

In the **first step**, the state estimate and covariance are mixed. These mixed estimates and covariances are the inputs of the Kalman filter. The equations are [15]:

$$U_{ij,k-1} = \frac{P_{ij} u_{i,k-1}}{\sum_{i=1}^r P_{ij} u_{i,k-1}} \quad (3)$$

$$X_{j,k-1}^0 = \sum_{i=1}^r X_{i,k-1}^+ U_{ij,k-1}$$

$$P_{j,k-1}^0 = \sum_{i=1}^r U_{ij,k-1} \{P_{i,k-1}^+ + [X_{i,k-1}^+ - X_{j,k-1}^0][X_{i,k-1}^+ - X_{j,k-1}^0]^T\} \quad (5)$$

where indexes i, j and l indicate the different Kalman filters. Different dynamic Kalman filter models are used here, the total for u_i, X_j^0, X_i^0, P_j^0 and P_i^+ is r , total number for U_{ij} and p_{ij} is r^2 , where $u_{i,k-1}$ represents the probabilities of the model in the previous time interval (iteration) $k-1$.

Since the initial probabilities of the model have little effect on the results over time, they can be favorably selected. In this project, the initial probabilities of the model are placed in rectangular functions, where P_{ij} is element of the Markov transitional matrix, p_{ij} is probability that the target will pass from the model i to the model j in each time interval, U_{ij} represents the conditional probability of a target in the condition j -th model, which is crossed over state i -th model. The performance of the IMM algorithm is very dependent on the choice of the transition matrix, $X_{i,k-1}^u$ and $P_{i,k-1}^u$ represent the updated state vector and noise covariance, respectively, from the Kalman filter in the previous time

$k-1$, $X_{i,k-1}^0$ and $P_{i,k-1}^0$ are mixing state and error covariance, for each Kalman filter, as inputs in the time interval .

In the **second step**, multiple Kalman filter models are implemented (for each assumed dynamic motion model). The Kalman filter prediction step is given by the following equations:

$$\begin{cases} X_{j,k}^p = F_j \cdot X_{j,k-1}^0 \\ P_{j,k}^p = F_j \cdot P_{j,k-1}^0 \cdot F_j^T + Q_j \end{cases} \quad (6)$$

while the Kalman filter update step may be represented as:

$$\begin{aligned} K_j &= P_{j,k}^p \cdot H_j^T (H_j \cdot P_{j,k}^p \cdot H_j^T + R_j)^{-1} \\ X_{j,k}^m &= X_{j,k}^p + K_j \cdot (Z_k - H_j \cdot X_{j,k}^p) \\ P_{j,k}^m &= (I - K_j \cdot H_j) \cdot P_{j,k}^p \end{aligned} \quad (7)$$

where j indicate the ordinal number of the Kalman filter, F_j is dynamic filter model matrix, Q_j is noise process covariance, $X_{j,k}^p$ and $P_{j,k}^p$ are predicted state and error covariance, respectively, H_j is the measurements matrix R_j is measurements noise covariance, K_j is the Kalman gain, Z_k is the measurements from time interval k , I is identity matrix, $X_{j,k}^u$ and $P_{j,k}^u$ are updated state and error covariance, respectively.

In the **third step** we have updated a model probability as follows:

$$\begin{cases} S_{j,k} = H_j \cdot P_{j,k}^p \cdot H_j^T + R_j \\ \tilde{y}_{j,k} = Z_k - H_j \cdot X_{j,k}^p \end{cases} \quad (8)$$

$$\begin{cases} d_{j,k}^2 = \tilde{y}_{j,k}^T \cdot S_{j,k}^{-1} \cdot \tilde{y}_{j,k} \\ \Lambda_{j,k} = \frac{1}{\sqrt{|2\pi \times S_{j,k}|}} \cdot \exp\left[-\frac{d_{j,k}^2}{2}\right] \end{cases} \quad (9)$$

$$u_{j,k} = \frac{u_{j,k-1} \cdot \Lambda_{j,k}}{\sum_{l=1}^r u_{j,k-1} \cdot \Lambda_{l,k}} \quad (10)$$

where index j is an ordinal number of the Kalman filter, $||$ is determinante of the matrix. Λ_j is likelihood function, $u_{j,k}$ is probability of a new model in time interval k .

In the **fourth and final step**, the state vector predictions are updated $X_{j,k}^u$ and error covariance $P_{j,k}^u$ from the Kalman filters are combined to obtain the final state and covariance of the trace error. The weighting factor is the likelihood of a new target movement model $u_{j,k}$:

$$X_k = \sum_{j=1}^r X_{j,k}^u \cdot u_{j,k} \quad (11)$$

$$P_k = \sum_{j=1}^r u_{j,k} \left\{ P_{j,k}^u + [X_{j,k}^u - X_k][X_{j,k}^u - X_k]^T \right\} \quad (12)$$

where X_k and P_k are combined state and error covariance of the tracks for l to r -th Kalman filter. Using the equations (1-9), the *IMM* state estimator calculates state and error covariance from time interval $k-1$ totime interval k .

PDAF step

The probabilities are used to measure the correction and covariance in a PDA filter. The basic assumptions and theories for the PDA filter can be found in [6, 7]. Here is a brief introduction of its functions and equations. The first step is to predict the trace state and covariance of the system error. Since the PDA filter is based on the Kalman filter, the first equations are for the prediction step and are the same as for the Kalman filter [16]:

$$X_{j,k}^p = F_j X_{j,k-1}^u \quad (13)$$

$$\begin{cases} \hat{z}_{j,k} = H_j \cdot X_{j,k}^p \\ P_{j,k}^p = F_j \cdot P_{j,k-1}^u \cdot F_j^T + Q_j \end{cases} \quad (14)$$

where j is an ordinal number of the *PDA* filter, $X_{j,k-1}^u$ is vector state in time interval $k-1$, F -dynamic model, $X_{j,k}^p$ - predicted state in time interval k , H -measurements matrix, $\hat{z}_{j,k}$ -predicted measurements state in time interval k , $P_{j,k-1}^p$ -error covariance in time interval $k-1$, Q_j is th noise process covariance.

In the second *PDA* step, we have performed the measurements which are used for update vector state and error covariance:

$$\begin{cases} v_{ij}^k = z_{i,k} - \hat{z}_{j,k} \\ S_{j,k} = H_j \cdot P_{j,k}^p \cdot H_j^T + R_j \end{cases} \quad (15)$$

$$(v_{ij}^k)^T \cdot S_{j,k} \cdot v_{ij}^k \leq \gamma \quad (16)$$

$$\begin{cases} V_j^k = \frac{4\pi}{3} \gamma^{3/2} \sqrt{|S_{j,k}|} \\ L_{i,j}^k = \frac{N[z_{i,k}; \hat{z}_{j,k}; S_{j,k}] \cdot P_D}{m/V_j^k} \end{cases} \quad (17)$$

$$\beta_{ij}^k = \begin{cases} \frac{L_{ij}^k}{1 - P_D \cdot P_G + \sum_{n=1}^m L_{n,j}^k}, i = 1, \dots, m \\ \frac{1 - P_D \cdot P_G}{1 - P_D \cdot P_G + \sum_{n=1}^m L_{n,j}^k}, i = 0 \end{cases} \quad (18)$$

where j is an ordinal of the *PDA* filters, V_j^k is volume region of validation, m is a total number of measurements in

the region of validation, $N[z_{i,k}; \hat{z}_k; S_k]$ is a normal distribution with variance S_k , L_{ij} is likelihood of the i -th measurements for the j -th PDA filter, β_{ij} is a probability of association of the i -th measurements for the j -th PDA filter, P_D and P_G are detection and gate probability of target respectively, β_i^k is a probability of association for confirmed measurements. Here β_0^k is a probability for non-valid measurements.

Proposed value for P_D и P_G can be given in [5]. Probability of detection P_D is often greater than 90% for the surveillance radar and 98% for the secondary radar. The last step is an update vector state and covariance of track. In this step, only confirmed measurements and their probability of association are used.

$$\begin{cases} \zeta_{j,k} = \sum_{i=1}^{m_k} \beta_{i,j} \cdot Z_{i,k}^j \\ W_{j,k} = P_{j,k}^p \cdot H_j^T \cdot (S_{j,k})^{-1} \end{cases} \quad (19)$$

$$\begin{cases} P_{j,k}^j = P_{j,k}^p - W_{j,k} \cdot S_{j,k} \cdot W_{j,k}^Y \\ P_{j,k}^j = W_{j,k} \left[\sum_{i=1}^{m_k} \beta_{i,j} \cdot Z_{i,k}^j - \zeta_{j,k} \cdot \zeta_{j,k}^T \right] W_{j,k}^T \end{cases} \quad (20)$$

$$\begin{cases} X_{j,k}^u = X_{j,k}^- + W_{j,k} \cdot \zeta_{j,k} \\ P_{j,k}^u = \beta_0^j \cdot P_{j,k}^p + (1 - \beta_0^j) \cdot P_{j,k}^j + P_{j,k}^j \end{cases} \quad (21)$$

where j is an ordinal number of the PDA filter.

Results of Simulations

The application selected for the study was a two-dimensional (positions and velocities), four-state aircraft tracking problem in which the sensor observes both position coordinates. The false measurements satisfied a Poisson distribution with density $\rho = 10^{-4}$ [scan/m²]. Both dimensions were assumed independent, and the sensor measurement errors, target maneuver state excitation errors, and the equations of motion were assumed identical in each dimension.

For the purpose of the simulation, the scenario with six (Fig.5) and twenty targets has been selected (Fig.8). Two diagrams are used to compare the quality of tracking:

- a comparative diagram of the number of simulated targets and the number of realized tracks,
- a diagram of the root mean square error (RMSE).

Tracks are initialized by each pair of measurements in consecutive scans, so that they meet the maximum speed criterion provided they are not selected from any other trace. Each new initialized trace is assigned an initial detection probability, which is described in detail in the literature [13]. In this way, if the target is not tracked by the track, a new track is initialized using its detections. The track can start following the same target, or the same measurement sequence. When this

happens, the estimation of the state of the trajectory should converge, and these tracks will be united. In each scan, a number of false tracks are initialized. In that situation, the first thing the tracking algorithm should do is discriminate or separate between the real and false tracks [18, 19].

The false track rejection procedure uses “track quality measurements” to eliminate tracks of “poor” quality and is presumed to be false, while at the same time confirming “high” quality tracks and calling them real.

The analysis of the impact of probability of detections versus signal to noise ratio (where probability of the false alarm is a parameter) was conducted in Fig.4. For the value SNR ratio 13.2dB, given empirical from CA CFAR and CATM CFAR), we calculate the detection of probabilities $P_D=0.6$ and $P_D=0.87$, respectively.

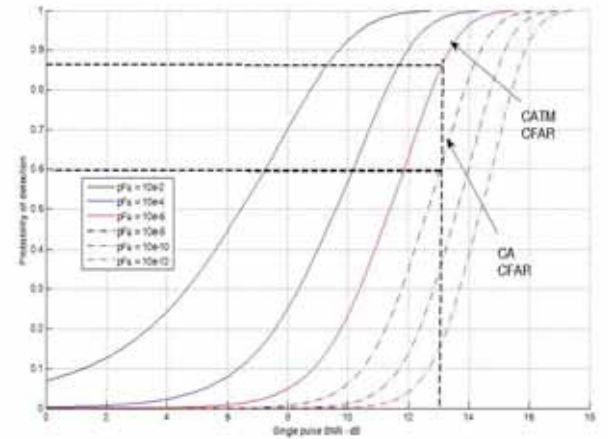


Figure 4. Parametric diagrams probability of detections versus signal to noise ratio (parameter probability of the false alarm)

Six targets scenario

Six targets are moving straight or with a maneuver (Fig.5). The sampling period of the radar sensor is $T=1$ s. Duration of the scenario is 50 scans. The target moves in the region $x=[0; 1000]$, $y=[0;500]$ and can appear or disappear in the scene at any time. The target states consist of positions and velocities and move according to the linear and Gaussian target dynamics [20]. Comparative diagram of simulated and realized tracks (six targets) is given in Fig.6.

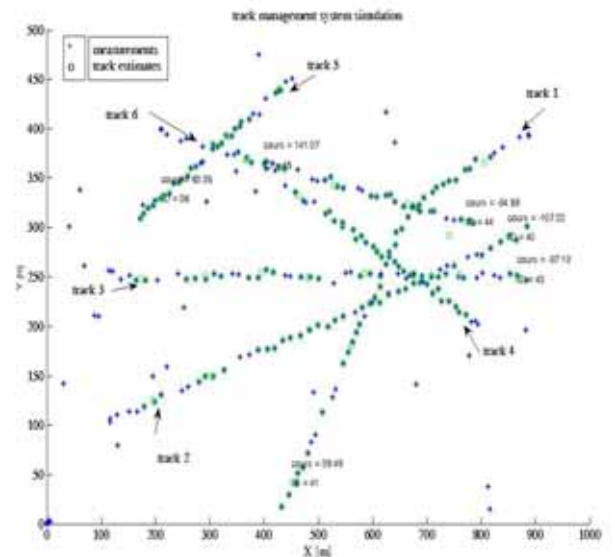


Figure 5. Simulations scenario of six targets

Comparative diagram RMSE of the position for overall (six) tracks (CATM CFAR versus CA CFAR) is given in Fig.7.

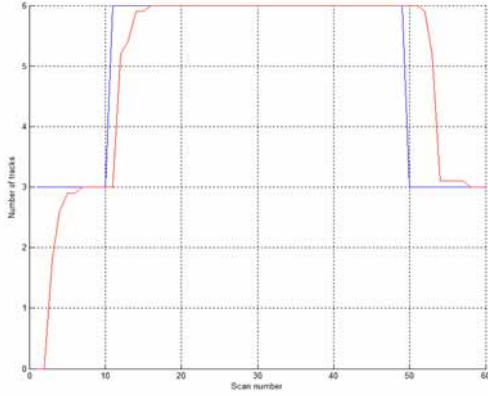


Figure 6. Comparative diagram of simulated and realized tracks (six targets)

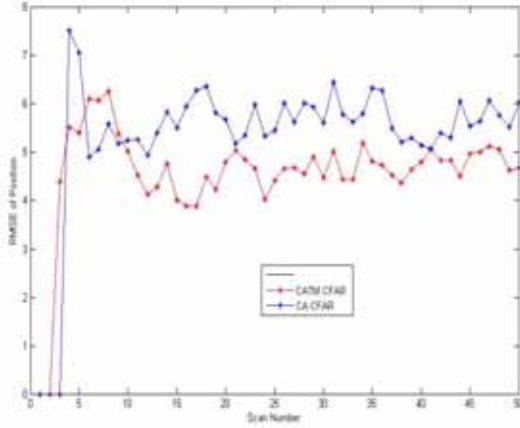


Figure 7. Comparative diagram RMSE of the position for overall tracks (CATM CFAR versus CA CFAR)

The system input is modeled as follows: $X = [x \ \dot{x} \ y \ \dot{y}]$ is a vector state, x, y are the Cartesian coordinates of the target position, \dot{x}, \dot{y} are the appropriate velocities. Transition matrix (F_{CV} - constant velocity model and F_{CT} - coordinate turn model) and process noise matrix are given by:

$$F_{CV} = \begin{bmatrix} 1 & T & 0 & 0 \\ 0 & 1 & 0 & 0 \\ 0 & 0 & 1 & T \\ 0 & 0 & 0 & 1 \end{bmatrix} \quad (22)$$

$$F_{CT} = \begin{bmatrix} 1 & \frac{\sin(\omega t)}{\omega} & 0 & \frac{\cos(\omega t) - 1}{\omega} \\ 0 & \cos(\omega t) & 0 & -\sin(\omega t) \\ 0 & \frac{1 - \cos(\omega t)}{\omega} & 1 & \frac{\sin(\omega t)}{\omega} \\ 0 & \sin(\omega t) & 0 & \cos(\omega t) \end{bmatrix} \quad (23)$$

$$Q(k) = q \begin{bmatrix} T^3/3 & T^2/2 & 0 & 0 \\ T^2/2 & T & 0 & 0 \\ 0 & 0 & T^3/3 & T^2/2 \\ 0 & 0 & T^2/2 & T \end{bmatrix} \quad (24)$$

Twenty targets scenario

Twenty targets are moving straight or with a maneuver (Fig.8). The sampling period of the radar sensor is $T=1s$. Duration of the scenario is 50 scans. The target moves in the region $x=[-40000;40000]$, $y=[-40000;40000]$ and can appear or disappear in the scene at any time. The target states consist of positions and velocities and move according to the linear and Gaussian target dynamics.

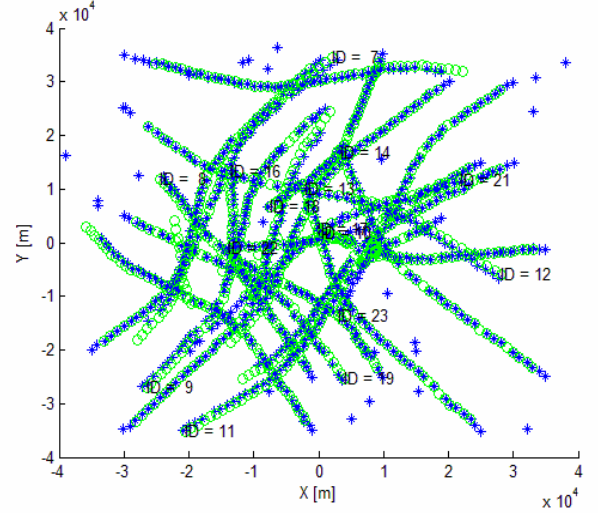


Figure 8. Simulations scenario of twenty targets

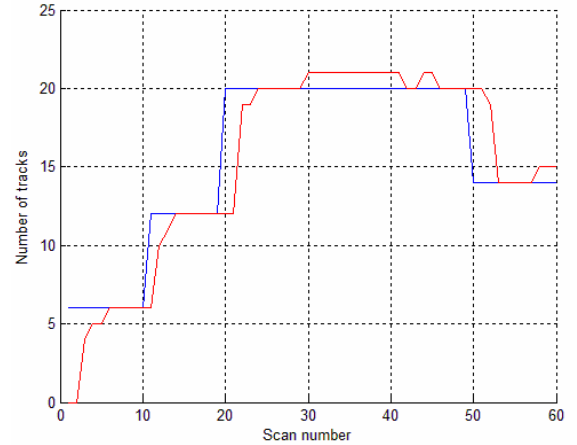


Figure 9. Comparative diagram of simulated and realized tracks (twenty targets)

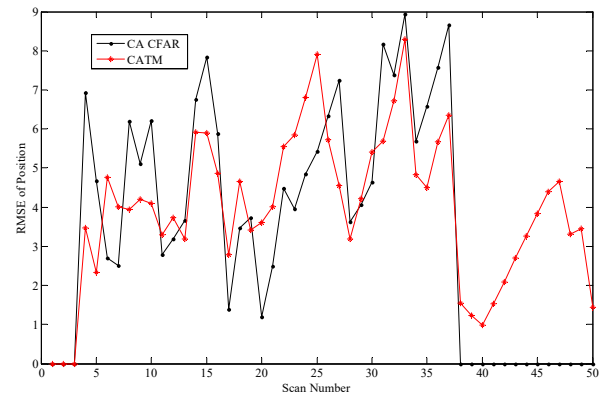


Figure 10. Comparative diagram RMSE of the position for overall (twenty) tracks (CATM CFAR versus CA CFAR)

The comparative diagram RMSE of the position for overall (twenty targets) tracks (CATM CFAR versus CA CFAR) is given in Fig.9. Finally, the comparative diagram RMSE of the position for overall (twenty) tracks (CATM CFAR versus CA CFAR) is given in Fig.10

Conclusion

The results of the study of the contribution of different types of CFAR detectors on the characteristics of the multi target tracking were given in the paper. The application of the CA CFAR and CATM CFAR algorithms in the radar pre-processing phase and their influence on the distribution of the clutter were examined, through the scattering of the actual confirmed traces in the known IMM PDAF algorithm.

The result of multi target tracking simulations, with six and with twenty targets, showed better tracking performance by the use of the CATM-CFAR algorithm, related to CA CFAR algorithm.

References

- [1] BLACKMAN,S.: Multiple-target tracking with radar applications. Artech House, 1986.
- [2] IVKOVIĆ,D., ANDRIĆ,M., ZRNIĆ,B.: *Detection of Very Close Targets by Fusion CFAR Detectors*, Scientific Technical Review, ISSN 1820-0206, 2016, Vol.66, No.3, pp. 50-57.
- [3] ROHLING,H.: *Radar CFAR Thresholding in Clutter and Multiple Target Situations*, IEEE Transaction on Aerospace and Electronic Systems Vol. AES-19, 1983, no.4, pp. 608-621.
- [4] FINN,H.M., JOHNSON,R.S.: *Adaptive detection mode with threshold control as a function of spatially sampled clutter level estimate*, RCA Rev., 1968, 29, (3), pp. 414-464.
- [5] TRUNK,G.V.: *Range resolution of targets using automatic detectors*, IEEE Transaction on Aerospace and Electronic Systems, 1978, 14, (5), pp.750-755.
- [6] IVKOVIĆ,D., ANDRIĆ,M., ZRNIĆ,B., OKILJEVIĆ,P., KOZIĆ,N.: *CATM-CFAR Detector in the Receiver of the Software Defined Radar*, Scientific Technical Review, ISSN 1820-0206, 2014, Vol.64, No.4, pp. 27-38.
- [7] REID,D.B.: *An algorithm for tracking multiple targets*, IEEE Transaction on Automatic Control, vol. 24, no. 6, 1979, pp. 843-854.
- [8] SINGER,R.A.: *Estimating optimal tracking filter performance for*
- [9] BLOM,H.A.P., BAR-SHALOM,Y.: *The interacting multiple model algorithm for systems with Markovian switching coefficients*, IEEE Trans. Automat. Contr. 1988, 33, pp. 780-783.
- [10] CHALLA,S., EVANS,R., MORELANDE,M., MUŠICKI,D.: *Fundamentals of Object Tracking*, Cambridge University Press, 2011.
- [11] MUŠICKI,D., EVANS,R., STANKOVIĆ,S.: *Integrated Probabilistic Data Association (IPDA)*, IEEE Transaction on Automatic Control, vol. 39, no. 6, 1994, pp. 1237-1241.
- [12] WELCH,G.; BISHOP,G.: *An Introduction to Kalman Filter*; Department of Computer Science University of North Carolina: Chapel Hill, NC, USA, 2006.
- [13] JAN,S.S., KAOY,C.: *Radar Tracking with an Interacting Multiple Model and Probabilistic Data Association Filter for Civil Aviation Applications*, Sensors 2013, 13, 6636-6650; doi:10.3390/s130506636
- [14] MUŠICKI,D., EVANS,R.: *Joint Integrated Probabilistic Data Association – JIPDA*, IEEE Transaction on Aerospace and Electronic Systems, vol. 40, 2004, no. 3, pp. 1093-1099.
- [15] SONG,T.L., MUŠICKI,D., KIM,D.S., RADOSAVLJEVIĆ,Z.: *Gaussian mixtures in multi-target tracking: a look at Gaussian Mixture Probability Hypothesis Density and Integrated Track Splitting*, IET Proceedings: Radar, Sonar and Navigation, vol. 6, 2012, no. 5, pp. 359-364.
- [16] RADOSAVLJEVIĆ,Z., MUŠICKI,D.: *Limits of target tracking in heavy clutter*, ASIA-Pacific International Conference of Synthetic Aperture Radar APSAR 2011, Seoul, Korea, 2011.
- [17] KOVACEVIC,B., IVKOVIC,D., RADOSAVLJEVIC,Z.: *IMMPDAF Approach for L-Band Radar Multiple Target Tracking*, Proceedings of 19th International Symposium INFOTEH-JAHORINA, 18-20 March 2020.
- [18] RADOSAVLJEVIC,Z., IVKOVIC,D.: *An Approach of Track Management System in Software Defined Radar*, Scientific Technical Review, 2018, Vol.68, No.1, pp. 73-80, Belgrade 2018, UDK 681:5.017:623:746.3
- [19] RADOSAVLJEVIC,Z.: *IPDA Filters in the Sense of Gaussian Mixture PHD Algorithm*, Scientific Technical Review, 2016, Vol.66, No.3, pp.34-40, Belgrade 2016, UDK : 681:5.017:623:746.3, COSATI:17-09, 12-01.
- [20] RADOSAVLJEVIC,Z., SONG,T.L., KOVACEVIC,B.: *Linear Multi-Target IPF Algorithm for Automatic Tracking*, Scientific Technical Review, 2016, Vol.66, No.1, pp.3-10, Belgrade 2016.

Received: 21.01.2021.

Accepted: 09.03.2021.

Pristup odnosa konstantnih lažnih alarma za poboljšano praćenje ciljeva

Svaki radar ima funkciju nadzora određenog područja od interesa. Radar takode ima funkciju praćenja pokretnih ciljeva na tom području sa izvesnom verovatnoćom otkrivanja, što zavisi od vrste detektora. Odnos konstantnih lažnih alarma (CFAR) je vrsta veoma često korišćen detektor. Promena verovatnoće otkrivanja ciljeva može direktno uticati na kvalitet praćenja pokretnih ciljeva. U radu su predstavljene teorijske osnove uticaja CFAR detektora na kvalitet praćenja, kao i pristup odabiru CFAR detektora CATM, koji omogućava bolje praćenje algoritmom Interaktivnog višestrukog modela (IMM) sa dva modela kretanja. Uredna analiza CA i CATM algoritma realizovana numeričkim simulacijama pokazala je da CATM CFAR daje manje grešaka u praćenju s proporcionalno istim računarskim resursima

Ključne reči: CFAR detektor, radarska detekcija, IMM, praćenje ciljeva